JOURNAL OF CATALYSIS 152, 415–418 (1995)

NOTE

Mercury Porosimetry Compacts SiO_2 Polymerization Catalysts

The pore size distribution (PSD) of catalysts is typically characterized by nitrogen sorption and mercury intrusion porosimetry. For most catalysts, the two techniques agree well in their overlap range from about 50 to 500 Å. However for many industrial and laboratory prepared SiO_2 ethylene polymerization catalysts, there exist considerable differences in the PSDs deduced from the routine application of the Kelvin and the Washburn equations to the nitrogen desorption and the Hg intrusion volume data, respectively (Fig. 1). This note will attribute the disagreement to the mechanical compression of the catalyst sample caused by the high pressures inherent in the use of mercury porosimetry. Such effects are well recognized for soft materials such as coals (1). Compression of silica polymerization catalysts during Hg porosimetry was first reported by Brown and Lard (2) in 1974; however, subsequent published PSDs for these catalysts did not mention the observation or deduction of compaction effects during mercury porosimetry (3). The report of Brown and Lard does not seem to have been widely disseminated, as the role of Hg porosimetry in compacting polymerization catalysts was independently rediscovered by Minihan *et al.* (4). Our observations are similar to those of the two previous studies (2, 4), but our data analysis shows how the compression can be used to characterize the mechanical properties of the catalysts.

The nitrogen desorption data were collected with a commercial instrument (Micromeritics ASAP 2400), analyzed with an algorithm similar to the BJH method, and then smoothed. The Hg intrusion was performed continuously (with a Quantachrome instrument); the intrusion data did not vary materially with the rate of intrusion. The data were analyzed with the Washburn model which assumes that the pores are cylinders whose diameter is given by

$$D = -4\sigma \cos \theta / p,$$

where D is the diameter, p is the pressure, σ is the surface tension of mercury (473 dynes/cm), and θ is the contact angle (140°). The Hg PSDs shown in the figures have a significantly higher level of smoothing than that used for the nitrogen desorption data.

As the pressure is increased, a number of sequential mechanisms increase the volume of mercury that enters the experimental cell containing the particles of porous material. Initially, at low absolute pressures, the particles in the cell (particularly if small) may be brought closer together; then the mercury will enter the spaces between the particles, and at higher pressures, the mercury will begin intruding into the pores of the individual particles, at a pressure determined by the Washburn equation. However, this implicitly assumes that the pores of the material remain unchanged as the Hg pressure is increased. For highly elastic materials with small pores, such as silicas with a total pore volume greater than 1 cm^3/g, the pore diameters decrease continuously with increasing porosimeter pressure. Thus the Hg will require a pressure significantly higher to enter a given pore than that expected from the low-pressure nitrogen sorption measurements: significant deviations will be observed between the PSDs measured by porosimetry and nitrogen sorption. For some materials, including commercial polymerization catalysts, the rate of pore size reduction due to particle compaction is high enough that the mercury *never* enters the pore spaces, within the pressure limitations of commercial instruments.

A typical mercury intrusion plot for commercial polymerization catalyst A (along with the corresponding nitrogen desorption PSD) is shown in Fig. 1. As is commonly practiced in analytical laboratories, the abscissa is the deduced Washburn pore diameter, rather than the measured mercury pressure. For Fig. 1, such a routine interpretation of the data would indicate a peak in the PSD at 90 Å (D_{Hg}) with a relatively flat distribution of pores up to 1200 Å. The nitrogen sorption PSD, also shown in Fig. 1, differs considerably from the mercury PSD, peaking at 220 Å (D_{N_2}). Our alternative interpretation of the data of Fig. 1 demarcates the intrusion curve into three distinct and sequential regimes indicative of catalyst particle elastic compression (I), catalyst particle structural collapse (II), and, finally, mercury intrusion into the pore spaces of the catalyst particle (III). Some of the catalysts may show an additional compactive regime IIa, between regime II and III, to be discussed below. Note that in regimes I, II, and IIa the measured mercury volume increase is due solely to particle deformation rather than pore intrusion: the use of the Washburn equation is not appropriate. However, the Washburn equation is relevant in regime III, measuring the com-

0021-9517/95 $6.00

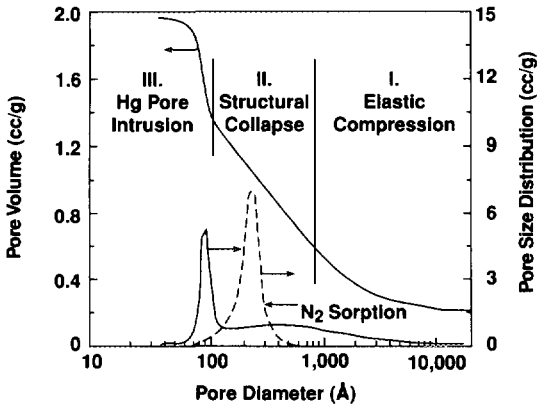

FIG. 1. Typical mercury intrusion curve and PSD (solid lines) and nitrogen desorption PSD (dashed line) for high volume polymerization catalysts (Catalyst A).

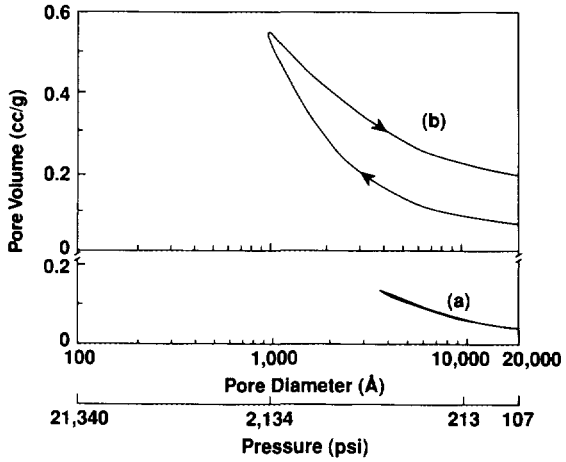

FIG. 3. (a) Reversibility of deformation in regime (I) for catalyst B. Volume changes during pressure increase and decrease are identical within instrument resolution. (b) Irreversible deformation when pressure is increased into regime (II) for catalyst B.

pacted pore diameters when the mercury does enter into the particles.

We have performed a number of tests to verify the validity of the above model. If region I is indeed due to elastic compression of the catalyst material, then the volume should plot linearly with pressure; furthermore, the deformation should be fully reversible with pressure decrease. Figures 2 and 3a support these expectations (catalyst B). Using the total pore volume of the material (1.7 cm^3/g as measured by nitrogen sorption) and the slope of the line in regime I (0.25×10^{-4} cm^3/g psi), the elastic bulk compressibility of the material is 1.5×10^{-5} psi^{-1}. After confirming the reversibility of the deformation, the catalyst was removed from the porosimeter for further inspection. Visually it retained its original milky white colour. We also checked for the possible presence of Hg within the catalyst particles by optical and electron microscopy (SEM and TEM); there was no such evidence.

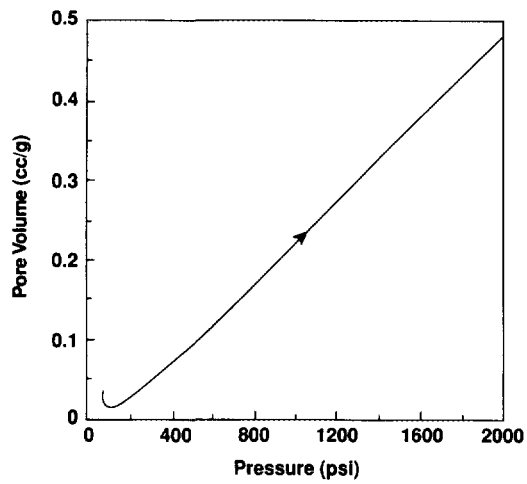

FIG. 2. Elastic regime (I) of catalyst B.

The "signature" for structural collapse of the catalyst is a linear region in the plot of the intruded volume vs log "diameter" (regime II), which actually is a linearity of intruded volume vs measured *pressure* (since the "diameter" is deduced from the pressure using the Washburn equation). Such a linearity between volume and log pressure is commonly observed when powders are compressed in a press. Here the volume changes occur by the breakage of the bonds between aggregations of elementary silica grains, and thus the volume changes in regime II should be substantially irreversible, in contrast to the reversible elastic regime (I). Figure 3b shows the irreversibility in the intrusion volume when the pressure is decreased after having being raised into region II. The sample was removed from the porosimeter and examined; visually it was still white, and optical, SEM, and TEM microscopy verified that no mercury entered into the pores.

A significant amount of compaction can occur in regime II, often with more than half of the total pore volume of the catalyst being lost. Since the pore diameters are approximately proportional to the ratio of the total pore volume to the total surface area (BET), the pore diameters can be expected to vary linearly with the total pore volume (since the BET surface area changes little with compaction). For a more detailed appreciation of the deformation caused by regime II, catalyst B's nitrogen desorption PSDs obtained prior to and subsequent to compaction were compared (Fig. 4). To achieve the compacted state, the porosimeter pressure was raised to 25,000 psi (Hg intrusion occurs at higher pressures), held there for 5 min, and reduced to atmosphere. The total pore volume of the catalyst (the area under the PSD

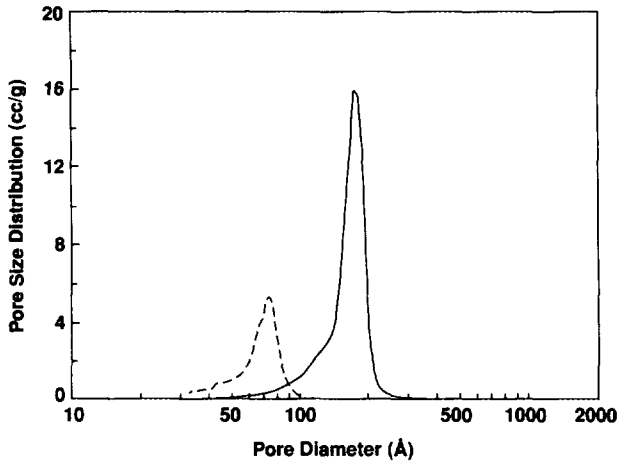

FIG. 4. Nitrogen desorption PSDs for catalyst B. The solid line (larger peak) represents the original PSD, while the dashed line represents the PSD after the sample had been exposed to 25,000 psi in the porosimeter cell. (For this sample, this pressure was not sufficient for Hg intrusion into the pores.)

curve) decreased from 2.1 to 0.76 cm^3/g, with the peak of the PSD decreasing from 167 to 71 Å. The shape of the PSD remains essentially log-normal. We see that the peak pore diameter is proportional to the total pore volume as suggested above.

Region III begins abruptly with a jump in the intrusion volume. This corresponds to the end of particle compaction and the intrusion of mercury into the pores that were previously being shrunk. After exposure to region III, the catalyst B particles were removed from the porosimeter and visually examined. The original milky white appearance of the catalyst particles, unchanged in regimes I and II, had now changed to dark gray/silver. Using the SEM in the X-ray energy dispersive mode verified the presence of Hg within the particles. The data of Fig. 1 indicate that region III begins when the combination of elastic and inelastic compression reduces the porosity of the particles from about 0.70 to nearly 0.25; i.e., the void spaces were reduced until the elementary spherical grains of SiO_2 were close packed. Further compression would have resulted in deformation of the grains from their essentially spherical shape.

For some catalysts with small SiO_2 grains, the catalyst particles enter and *remain* in a regime of grain deformation (IIa), with the mercury never entering the material pores within the pressure limitations of the instrument (60,000 psi). Upon inspection subsequent to such pressure exposure, the catalyst remains milky white in appearance. The slope of regime IIa indicates increased resistance of the material to volume change, as would be expected if the mechanism changes from the grain rearrangement of regime II to grain deformation.

It is commonly recognized that the pore morphology of supported polymerization catalysts influences both catalyst activity and polymer properties. Supports with high pore volumes and large average pore diameters tend to exhibit high polymerization activity and to produce lower molecular weight polymers. Despite the overwhelming empirical evidence connecting support morphology and friability with polymerization performance few quantitative relationships have been established. Part of the problem may be the routine interpretation of the mercury intrusion data. The interpretation proposed here provides us with a number of new metrics potentially useful in defining these relationships: elastic compressibility (dV/VdP) from the slope of regime I, inelastic compression constant from the slope of regime II, pressure at material failure (commencement of regime II), and differences between D_{N_2} and D_{Hg} (the peak diameters as obtained by nitrogen sorption and mercury porosimetry). These new metrics could prove to be useful complements to the ones currently used to characterize catalyst pore morphology and strength.

For example, high-temperature calcination of the polymerization catalysts or the supports causes significant changes in the mechanical properties of the materials. For commercial catalyst C, Table 1 shows that the material becomes stiffer (the compressibility as derived from regime I decreases) as the activation temperature is increased. Furthermore, the pressure at which mechanical failure ensues (the start of regime II) also increases with calcination temperature. The mechanical properties of polymerization catalysts must represent a balance of strength to maintain structural integrity during handling and activation and friability to support fragmentation and particle growth during polymerization. During polymerization, the catalyst particles deform due to *tension*, as resin accumulates in the pores, rather than compression; the trends, however, can be expected to be similar. Thus to commence fragmentation of the catalyst particles calcined at 800°C, the internal pore pressure caused by polymerization will likely need to be twice that required for particles calcined at 400°C.

TABLE 1

Effects of Calcination Temperature on Catalyst C Mechanical Properties

Calcination temperature (°C)	Compressibility of catalyst (psi^{-1})	Pressure at failure (psi)
250	0.63×10^{-4}	3300
400	0.53×10^{-4}	3050
600	0.36×10^{-4}	4400
800	0.26×10^{-4}	6100

The routine interpretation of mercury intrusion data by the Washburn equation may seriously misrepresent the PSD of silica polymerization catalysts; we recommend the use of nitrogen sorption data as much as possible, particularly for catalysts with a total pore volume in excess of 1.0 cm^3/g. Compression of the catalysts due to the high pressures used during mercury porosimetry is the primary cause of deviations of the Hg PSDs from those derived from nitrogen sorption measurements. The small pores of many silica catalysts delay mercury intrusion while significant elastic particle compression occurs; further compression results in largely inelastic structural collapse; finally, at sufficiently high pressures, mercury enters the highly compacted pores of the silica particles. Note that *most* of the mercury "intrusion" curve has nothing to do with the pore sizes of the catalyst: Compression/compaction of the catalyst may easily be misidentified for the existence of large pores. Other methods of measuring the presence of macropores need to be developed, since nitrogen sorption lacks sufficient resolution for pores larger than about 500 Å. This work agrees with the early qualitative deductions of Brown and Lard (2) and the recent observations of Miniham *et al.* (4). Though clearly a cause of significant distortions in mercury intrusion PSDs, the compression and structural compaction inherent in mercury porosimetry can be viewed as an opportunity to better characterize the all-important structural properties of polymerization catalysts.

ACKNOWLEDGMENTS

We thank Chevron Chemical Company for permission to publish this paper. R. Aviani, P. Wanzo, B. Cates, and D. Haller performed the mercury intrusion experiments; T. Rea and I. Chan provided the images. We are very grateful to them all.

REFERENCES

1. Friesen, W. I., and Mikula, R. J., *J. Colloid Interface Sci.* **120,** 263 (1987).
2. Brown, S. M., and Lard, E. W., *Powder Technol.* **9,** 187 (1974).
3. Weist, E. L., Ali, A. H., and Conner, W. C., *Macromolecules* **20,** 689 (1987).
4. Minihan, A. R., Ward, D. R., and Whitby, W., "The Colloid Chemistry of Silica," p. 341, ACS Advances in Chemistry Series, Vol. 234. American Chemistry Society, Washington, DC, 1994.

E. Steven Vittoratos[1]

Chevron Research and Technology Company
100 Chevron Way
Richmond, California 94802

P. R. Auburn

Chevron Chemical Company
Technology Department
1862 Kingwood Drive
Kingwood, Texas 77339

Received June 21, 1994; revised November 3, 1994

[1] To whom correspondence should be addressed.